



This is a repository copy of *Control over Energy Transfer between Fluorescent BODIPY Dyes in a Strongly Coupled Microcavity*.

White Rose Research Online URL for this paper:
<http://eprints.whiterose.ac.uk/134371/>

Version: Accepted Version

Article:

Georgiou, K., Michetti, P., Gai, L. et al. (3 more authors) (2018) Control over Energy Transfer between Fluorescent BODIPY Dyes in a Strongly Coupled Microcavity. *ACS Photonics*, 5 (1). pp. 258-266. ISSN 2330-4022

<https://doi.org/10.1021/acsp Photonics.7b01002>

Reuse

Items deposited in White Rose Research Online are protected by copyright, with all rights reserved unless indicated otherwise. They may be downloaded and/or printed for private study, or other acts as permitted by national copyright laws. The publisher or other rights holders may allow further reproduction and re-use of the full text version. This is indicated by the licence information on the White Rose Research Online record for the item.

Takedown

If you consider content in White Rose Research Online to be in breach of UK law, please notify us by emailing eprints@whiterose.ac.uk including the URL of the record and the reason for the withdrawal request.



eprints@whiterose.ac.uk
<https://eprints.whiterose.ac.uk/>

Control over energy transfer between fluorescent BODIPY dyes in a strongly-coupled microcavity

Kyriacos Georgiou,¹ Paolo Michetti,² Lizhi Gai,³ Marco Cavazzini,⁴

Zhen Shen³ and David G. Lidzey^{*,1}

¹Department of Physics and Astronomy, The University of Sheffield,
Sheffield S3 7RH, United Kingdom

²Institute of Theoretical Physics, Technische Universität Dresden, 01062 Dresden, Germany

³State Key Laboratory of Coordination and Chemistry, School of Chemistry and Chemical
Engineering, Nanjing University, Nanjing 210046, China

⁴Istituto di Scienze e Tecnologie Molecolari del Consiglio Nazionale delle Ricerche (ISTM-CNR),
via Golgi 19, I-20133 Milano, Italy

Abstract

Hybridization of two fluorescent BODIPY dyes in a microcavity is achieved by coupling different exciton transitions to the same cavity mode. We characterise the luminescence of such hybrid system following non-resonant laser excitation and show that the relative population along the different polariton branches can be controlled by changing cavity detuning. This effect is used to enhance exciton energy-transfer to states along the lower polariton branch in negatively detuned cavities. We compare the efficiency of energy transfer via exciton hybridisation with that achieved by dipole-dipole coupling.

KEYWORDS: polaritons, microcavities, hybridization, radiative pumping, fluorescent molecules

Since the first demonstration of strong coupling in organic microcavities in 1998¹ and room temperature polariton emission shortly after², organic exciton-polaritons have become a popular testbed for studying intriguing physics and macroscopic quantum phenomena at room temperature.³⁻⁸ Organic polariton condensation and lasing has been reported in a handful of different systems such as conjugated-polymers³, fluorescent proteins⁴, pure films of fluorescent molecules⁵ and crystalline organic semiconductors.⁶ Very recently, a room temperature organic exciton-polariton condensate was demonstrated in a cavity containing a fluorescent molecule dispersed in an inert polymer matrix.⁹ Achieving condensation in such dilute molecular systems opens the possibility to create polariton lasers having wavelengths spanning the entire visible and near IR. However, it is not yet obvious which properties of organic materials lead to efficient polariton condensation and lasing. Efficient population of polaritons towards the bottom of the lower polariton branch (LPB) appears to be a key component in generating a macroscopic occupation and bosonic final state stimulation.¹⁰ Understanding and controlling possible relaxation pathways is therefore an essential component in the design of efficient polariton lasing devices.

Hybridization of Frenkel excitons through strong coupling and polariton mediated energy transfer between different excitons has been demonstrated in microcavities containing J-aggregated cyanine dyes.¹¹⁻¹⁴ Such molecular aggregates have relatively narrow absorption linewidths (10s of meV)^{15,16}, allowing different materials to be selected whose excitonic transitions are separated by an energy commensurate with the typical Rabi-splitting energy of a molecular material in a microcavity (~ 100 meV).^{1,2,17} However many J-aggregated molecular dyes have low fluorescence quantum efficiency¹⁸ as a result of competing non-radiative pathways; a property that has so-far precluded polaritons in J-aggregate microcavities undergoing condensation and lasing. It is of great interest therefore to explore polariton hybridisation in microcavities based on diluted highly fluorescent molecules, as such materials have already been shown to undergo room temperature polariton condensation.⁹ We believe that by understanding and controlling energy transfer between hybridized molecular systems having high radiative rates, it may be possible to harness such effects to efficiently generate macroscopic polariton occupations in the 'energy-trap' at the bottom of the lower polariton branch and therefore reduce polariton lasing thresholds.

In this paper, we explore polariton hybridisation and energy transfer in hybrid cavities containing a combination of two different, highly fluorescent molecular dyes doped in an optically inert polymer matrix. In cavities containing cyanine-dye J-aggregates, energy-transfer between polariton states can occur that is mediated by hybridised middle-polariton branch (MPB) states.¹² Here, our objective is to explore whether such a process occurs in a cavity containing hybridised-fluorescent molecular dyes, and to compare the efficiency of such a process with the same structure in which direct energy transfer can occur between the dyes by dipole-dipole coupling (Förster transfer). In our experiments, we control direct and indirect interactions between uncoupled excitonic states by design of the cavity 'active' layer. In one type of microcavity (hereafter termed a 'multilayer cavity'), we place an optically inert thin spacer of the polymer polyvinyl-alcohol (PVA) between two active layers that both contain a different type of strongly-coupled molecular dye dispersed in a polystyrene (PS) matrix. Here, the thickness of the spacer layer was several tens of nm corresponding to a value well in excess of the typical Förster transfer radii (typically less than 10 nm).^{19,20} The spacer layer thus precludes any direct dipole-dipole coupling between molecules in the different active layers. In the second type of microcavity (termed a 'blend cavity'), the two different molecular dyes are instead mixed together in a polystyrene matrix, with the average spatial separation between molecules being < 3 nm, permitting direct dipole-dipole coupling and thus non-radiative energy transfer.²¹ Our experiments allow us to compare the efficiency of energy transfer in the strong-coupling regime against that of short-range Förster transfer. We show that energy transfer to states along the lower polariton branch is significantly enhanced in a negatively detuned cavity, however this process is not as efficient as dipole-dipole coupling in which energy-transfer occurs with an efficiency almost unity.

The molecular materials used in our experiments are based on a boron-dipyrrromethene core (BODIPY) that has been functionalised in such a way to modify its exciton energy (see Methods). The chemical structures as well as the optical absorption and fluorescence spectra of the two BODIPY derivatives (termed BODIPY-Br and BODIPY-R) as measured from control thin films is shown in Figure 1(a) and (b) respectively. Here spectra recorded when the dyes were dispersed in a PS matrix at a concentration of 20% and 10% respectively (by mass). BODIPY-Br has a (0,0) electronic transition at 530 nm that can strong-couple, which we refer to, for the sake of simplicity, as 'Br'. The

molecular dye BODIPY-R has two dipole-allowed transitions at 581 and 630 nm (corresponding to (0,1) vibronic and (0,0) electronic transitions) that we show can both undergo strong-coupling, which we refer to as 'R1' and 'R2' respectively.

BODIPY-Br and BODIPY-R were deposited into microcavity structures consisting of two silver mirrors (a 200 nm thick bottom mirror and a 35 nm thick semi-transparent top mirror deposited by thermal evaporation) with the whole structure fabricated on a quartz-coated glass substrate. To fabricate 'multilayer' cavities (see schematic in Figure 1(d)), a layer of PVA (spin-cast from a water solution) was used to separate the two BODIPY containing PS films that were both spin-cast from toluene. The orthogonal nature of the solutions used to deposit the various layers permitted well-defined and stable multilayers to be constructed. 'Blend' cavities instead contained a mixture of BODIPY-Br and BODIPY-R that were both dispersed in a PS matrix and deposited in a single layer. The optical properties of a (control) blend layer of BODIPY-Br and BODIPY-R and a multilayer of the same materials is shown in Figure 1(c).

We firstly consider the optical properties of the blend film. Here, we find that its measured absorption spectrum can be described by an approximate superposition of the absorption spectra of its BODIPY-Br and BODIPY-R components. This is shown in Figure 1(c) where we simulate the blend absorption based on a linear superposition of absorption spectra (19% BODIPY-Br and 11% BODIPY-R); a composition that is very similar to that added to the solution used to spin-cast this layer (20% BODIPY-Br and 10% BODIPY-R). This indicates that there is no direct ground-state interaction between the different molecular materials. However excited-state energy transfer between the BODIPY-Br and BODIPY-R components is highly efficient (see spectra plotted using a blue line); on excitation of the film at 473 nm, we find that 99% of PL emission comes from BODIPY-R, with this emission being slightly red-shifted in wavelength due to an inner-filter effect. We attribute the suppression of the BODIPY-Br PL from the blend film as resulting from dipole-dipole coupling between the two different molecular dyes, with BODIPY-Br acting as a donor and BODIPY-R as an acceptor.

The optical absorption of the multilayer can also be approximated by a superposition of the absorption spectra of its BODIPY-Br and BODIPY-R components. The PL emission from the multilayer is however qualitatively different from that of the blend film, with a similar intensity of emission from both BODIPY-Br and BODIPY-R observed (see spectra

plotted using a red-line in Figure 1(c)). We can in fact describe the emission spectrum of the multilayer using a weighted linear superposition of the emission spectra of its individual components. Here, by integrating the area under the fitted single components of the bilayer, we find that an equal fraction of emission originates from BODIPY-Br and BODIPY-R. In both the multilayer and blend configurations, we find that the PL emission spectrum is not apparently dependent on the side from which the multilayer film is initially excited.

We now consider the optical properties of blend and multilayer films when placed into a microcavity. Here, for each type of cavity, we have fabricated positively ($\Delta=+28$ meV) and negatively ($\Delta=-162$ meV) detuned cavities. Here, we define detuning by the energy difference between BODIPY-R exciton energy (E_R) and photon energy (E_p) at normal incidence where $\Delta = E_p - E_R$. This was done by adjusting the total film thickness to be 330 nm and 390 nm for the positively and negatively-detuned cavities respectively. To confirm optical strong coupling, we recorded the angular dependent white-light optical reflectivity of the different cavities. The reflectivity spectra of four cavities are plotted in Figure 2(a) to (d). Here parts (a) and (b) correspond to measurements made on positively and negatively detuned multilayer cavities (labelled as M_p and M_n respectively). Parts (c) and (d) similarly correspond to measurements made on positively and negatively detuned blend cavities (labelled as B_p and B_n respectively). In all cases, strong coupling is evidenced by anticrossing of the polariton branches at the angles where the photon mode and excitons would have been degenerate. As our cavities couple together four oscillators Br, R1, R2 and the cavity mode, we expect the cavity dispersion to be characterised by four polariton branches.

To model the cavities, we use a four-level coupled oscillator model (see Supporting Information), which on diagonalization of the Hamiltonian results in four unique solutions. These are fit to the polariton branches as shown in the reflectivity spectra of the cavities in Figure 2(a) to (d). We tabulate the energy of the LPB at $k_{//}=0$ and the coupling constants used in the fits in Supporting Information Table S1. We also identify the upper and lower polariton branches (UPB and LPB), as well as two middle branches (MPB1 and MPB2) in Figure 2, and also plot the energy of the uncoupled photon (P) and Br, R1 and R2 transitions. From the four-level coupled oscillator model, we determine the different Hopfield coefficients that quantify the exciton and photon mixing in each of

the cavity branches. This is plotted for the middle and lower polariton branches for M_p , M_n , B_p and B_n cavities as shown in Figure 3. For simplicity, we omit the upper polariton-branch in our discussions as the polariton population in such states is in most cases relatively low.

Note that the multilayer and the blend configuration cavities were designed to have identical optical properties. Whilst this was largely achieved (as indicated by the very similar cavity-mode dispersion curves), we find it was necessary to use slightly different values of background refractive index and coupling strength between excitons and photons in our modelling. There are two reasons for this; firstly the PVA layer has lower refractive index (1.50) compared to that of PS (1.59). As PVA was not used in the blend cavities, the effective refractive index used was slightly higher. Secondly, the blended cavities required a thicker active layer in order to compensate for the thickness and photon-exciton detuning, in the absence of the PVA spacer layer which then resulted in a slight increase of the coupling strength between the excitons and the cavity mode. As can be seen in Figure 3, the Hopfield mixing fractions are very similar in the different cavity pairs (M_p , B_p) and (M_n , B_n).

We have also used a transfer matrix model to calculate the distribution of the electric field ($|E^2|$) in the structures studied. Figure 4(a) to (d) shows calculated values of $|E^2|$ together with the refractive index of the different layers in a direction parallel to the cavity axis. In each cavity, we identify the location of the various layers (either dye-doped polystyrene layer or a PVA spacer layer). In the multilayer cavities (parts (a) and (c)), it can be seen that there are field antinodes in the middle of each of the active layers and a node in the centre of the PVA spacer. This field distribution results in efficient coupling between the excitons and the cavity mode. In the blend cavities (parts (b) and (d)), the active materials are distributed through a single layer, with the distribution of the field being qualitatively very similar.

We have explored angular PL emission from the cavities following non-resonant excitation at 500 nm (see Fig. 5(a) to (d)). Here, excitation was performed close to normal incidence, with luminescence collected using a lens mounted on one arm of a goniometer and then delivered to a CCD spectrometer via a fibre-optic bundle. We estimate that the lens collected luminescence over a solid angle of 0.05 sr and a range of angles between 0 and 70°. It can be seen that in the multilayer cavities, PL is mainly

emitted by the MPB1 and MPB2 in the positively detuned cavity (see Fig. 5(a)), and by the LPB in the negatively detuned cavity (see Fig. 5(c)). In contrast, PL emission from the blend cavities comes only from the LPB in both positively and negatively detuned cavities (see Fig. 5(b) and (d)). We note that the emission distribution from the negatively detuned multilayer cavity is qualitatively similar to that observed previously in strongly-coupled microcavities containing two hybridized J-aggregated cyanine dyes.¹²

To analyse data shown in Figure 5 in a quantitative manner, and convert intensity of luminescence into a relative polariton population, we need to correct for both the photon-fraction of each emissive state, and also the relative angle subtended by our angular measurement process. We discuss this correction in Supplementary Information. In brief, we convert the intensity of luminescence from each of the branches measured at any angle ($I(\theta)$) to a relative polariton population density ($f_k(\theta)$) using $f_k(\theta) = I(\theta)/[|\alpha_\gamma(\theta)|^2 \cos(\theta) |E_p(\theta)|^2]$ where $E_p(\theta)$ is the energy of the polaritons and $|\alpha_\gamma(\theta)|^2$ is the photon fraction of the branch. We then integrate $f_k(\theta)$ over all angles, to determine the total polariton population along each of the polariton branches. Figure 6(a) to (d) plots $f_k(\theta)$ for the middle and lower polariton branches for cavities M_p and M_n (parts (a) and (c)) and the lower branch in cavities B_p and B_n (parts (b) and (d)) respectively. Note that the middle branch polariton population in cavities B_p , and B_n is not plotted as it is negligible. We discuss the relative population of states along these different branches in the following paragraphs.

We have previously shown that the LPB in BODIPY-Br cavities can be effectively populated following radiative decay of weak-coupled excitons in an exciton reservoir (positioned at lower-energy) that populates (pumps) the photonic component of the polariton. This process is maximised for photon-like polariton states. Note however, our previous measurements have shown the distribution of weak-coupled exciton reservoir states is not simply defined by the total distribution of emissive excitonic states.²² Rather in BODIPY-Br cavities, it appears that emission from a combination of weak-coupled excimer states, together with vibronic emission from (0,1) excitons is most effective in pumping LPB polariton states. Here, we use such a concept to understand the emission from hybrid polariton cavities.

We first consider the positively detuned multilayer cavity (M_p). Here, non-resonant excitation of the cavity only seems effective in populating MPB states. This observation can be partly explained using the Hopfield coefficients for MPB1,2 as determined using the coupled oscillator model as can be seen in Figure 3(a) and (b). Here, we find that the MPB1 and MPB2 are highly photon-like over a range of angles, with MPB2 consisting of a relatively large fraction of Br at large angles. As the efficiency of the photon-pumping mechanism is proportional to the photon-fraction of the polariton branch, we expect MPB1 and MPB2 polaritons to be efficiently pumped by the weakly-coupled excitons in the Br reservoir. Our previous measurements on BODIPY-Br cavities have shown that this reservoir is most effective in optically pumping polariton states over the wavelength range 570 to 600 nm.²² The coincidence between the spectral position of the two middle branches in cavity M_p (542 to 615 nm) and the Br exciton reservoir qualitatively suggests that weak-coupled Br states should be able to optically pump hybrid middle-branch polariton states. Figure 6(a) confirms the effective population of MPB states by the substantial polariton population that is determined along these branches (particularly at high angle corresponding to energies close to the Br exciton reservoir).

The polariton population on the LPB of cavity M_p is in contrast much lower (again see Fig. 6(a)). There are a number of effects that we believe contribute to this result. Firstly, the highly radiative nature of the middle branches in this cavity means that polaritons on MPB1,2 are more likely to decay via photon emission, rather than undergo relaxation to the BODIPY-R reservoir. Secondly, the positive detuned nature of this cavity means that the bottom of the LPB is positioned close in energy to the BODIPY-R (0,0) exciton (within 50 meV). We have previously shown in a strong-coupled BODIPY-Br cavity that the LPB is actively populated 250 meV below the (0-0) exciton resonance by a radiative scattering process, which we associated with vibronic-assisted (0-1) radiative emission or/and with the presence of low-lying weakly-coupled exciton states (i.e. 250 meV below the (0-0) resonance).²² If we assume a similar behavior for the BODIPY-R system, then we would expect a radiative pumping mechanism active at about 720 nm, which is however far below the bottom of the LPB of the M_p microcavity. Previous theoretical and experimental work has shown that such vibronic emission is able to efficiently pump polaritons on the LPB.²²⁻²⁴ However as the bottom of the LPB in the M_p cavity is located at 644 nm, we speculate that there is not a sufficient reservoir population

available at this wavelength to populate LPB polaritons. Note that the LPB in this cavity is also predominantly exciton-like (see Figure 3(a)), with its photon-fraction that rapidly decreases at higher angles also suppressing possible radiative scattering processes.

We now discuss the negatively detuned multilayer cavity M_n (see Fig 3(c)). Here, we find that the LPB is highly photon-like particularly at small angles (84% at normal incidence) and emits luminescence efficiently as shown in Figure 5(c). Figure 6(c) confirms that the polariton population in the LPB is also greater than that of MPB1,2 (between angles of 0 and 26°). The LPB is now in the correct energy range for the radiative scattering mechanism from the BODIPY-R reservoir to take place; indeed, the bottom of the LPB is located around 710 nm, providing a very effective route to populate polaritons on the LPB.

In contrast to M_p , the emission from MPB1 in cavity M_n is suppressed (see Fig 5(c)). Here we expect the two middle branches to be efficiently pumped from the BODIPY-Br reservoir, with the general increase in population on MPB1,2 at angles $> 40^\circ$ consistent with a greater overlap with reservoir states. However MPB1 and MPB2 are likely to be significantly less radiant than the LPB, as they contain a lower photon fraction – see Fig 3(d). We suspect that polaritons on MPB1 are likely to scatter down in energy and populate the lower lying BODIPY-R reservoir as they contain a high R2 fraction. Such polaritons are then available to populate states along the LPB; a result confirmed by the distribution of polaritons along the different branches shown in Figure 6(c). Our measurements therefore suggest that negatively detuned hybrid-cavities are relatively more efficient in promoting energy transfer between the coupled states than comparable positively detuned structures.

We now turn our attention to the blend cavities B_p and B_n . In the non-cavity film of the blend, non-radiative energy transfer suppresses emission from the BODIPY-Br donor exciton and the BODIPY-R acceptor exciton is the only source of luminescence. As it has been discussed earlier for the multilayer cavities, radiative pumping appears to be the main mechanism by which polaritonic states are populated. We therefore expect that energy transfer into the low-lying BODIPY-R reservoir will suppress population of middle branch polaritons. This is indeed confirmed in Figure 5(b) and (d) that show the emission from cavities B_p and B_n is dominated by LPB luminescence. Indeed in these

cavities, the polariton population is distributed towards the bottom of the LPB (see Fig. 6(b) and (d)). The absence of luminescence from the middle branches confirms the fact that despite such states being energetically accessible, relaxation within the exciton reservoirs occurs more rapidly than excitons can populate states on MPB1 and MPB2. This result is consistent with previous studies on microcavities in which a cavity photon was strongly-coupled to the Soret-band of a porphyrin dye.¹ Here, it was found that the polariton states were non-luminescent due to rapid relaxation of excitons to the lower lying q-band.

We can use our measurements of the angular-dependent emission to explore the relative efficiency of the energy transfer process that is generated by exciton hybridization. Returning to Figure 6(a) and (c), we find that in cavity M_n 44% of total polariton states are found on the LPB with 12% and 44% of states located on MPB1 and 2 respectively. Notably however, both MPB1 and 2 contain a high BODIPY-R exciton fraction (see Fig 3(d)). If we now arbitrarily include polariton states along the middle-branches whose *excitonic component* is predominantly derived from BODIPY-R (i.e. having > 90% of their *excitonic fraction* being BODIPY-R), we find that around 85% of all *polariton states* in the cavity are in fact associated with BODIPY-R, indicating a substantial degree of population transfer. This is in direct contrast to cavity M_p in which only 6% of polaritons are located on the LPB, with 53% and 41% of polaritons located on MPB1 and 2 respectively. Here, while states along MPB1 contain a high fraction of BODIPY-R, polariton branch MPB2 contains a majority fraction (at angles greater than 40°) of BODIPY-Br. This indicates in cavity M_p , energy transfer is relatively suppressed.

Figure 6(b) and (d) indicates that in cavities B_n and B_p , all states are located on the LPB (which in both cavities contains a negligible fraction of BODIPY-Br). This indicates that Förster transfer is more efficient than energy-transfer mediated by exciton hybridization. However it is clear that polariton-hybridisation is able to transfer energy between excitonic states that are separated by much larger distances than could be achieved by direct dipole-dipole coupling (here the PVA spacer layer has a thickness of 60 nm). Our measurements also demonstrate that the level of energy transfer between polariton states is critically dependent on cavity design with the relative population of lower branch polaritons being around 6 times higher in cavity M_n compared to cavity M_p .

We can also evidence a significant redistribution in emission generated by hybridization of excitons in the strong coupling regime by comparing the integrated angular emission with that of a control film. To explore this effect, we have placed cavities M_n and M_p inside an integrating sphere, and have measured their emission following non-resonant excitation at 405 nm as shown in Figures 7(a) and (b) respectively. For comparison, we indicate the spectral regions that correspond to the various polariton branches using shaded blocks. Here, the difference in luminescence emission from the different cavities is apparent, with cavity M_n dominated by an emission band around 650 to 700 nm. Cavity M_p in contrast is characterized by emission that peaks at 556 nm. Comparing this data with the PL emission from the control multilayer film shown in Figure 1(c), it can be seen that both types of cavity result in a dramatic change in emission pattern.

We analyse the PL emission spectra by fitting it to a series of Lorentz curves. These curves are then integrated over wavelength to determine the percentage of emission corresponding to each polariton branch. Our calculation suggests that in the positively detuned multilayer cavity M_p , 12% of the total emission is emitted from the LPB with the remainder emitted from MPB1 and 2. In the negatively detuned cavity M_n , the LPB is highly emissive, and comprises 87% of total emission. This result again confirms that there is redistribution of luminescence towards states associated with BODIPY-R in negatively detuned cavities, while in the positively detuned cavities, emission mainly occurs at wavelengths corresponding to the emission from both MPB1 and 2 (which also closely coincides with the emission peak of BODIPY-Br).

In conclusion, we have studied strong-coupling and hybridization between the excitonic-transition of two organic dyes in two different cavity configurations; one that incorporated an inert spacer-layer to separate the two dye layers and the other containing the same dye-molecules that had been blended together in a host matrix. We show that in cavities containing the spacer layer, the emission pattern from the cavity is strongly dependent on the relative detuning of the cavity, with energy transfer to the lower polariton branch being significantly more efficient in a negatively detuned cavity compared to a positively detuned cavity. On placing the cavities into an integrating sphere, we determine that the negatively detuned cavity results in a strong redistribution of emission towards states associated with the lowest-energy excitonic state. We find however that energy transfer via strong coupling is not as an efficient

process as direct dipole-dipole coupling; here energy transfer between the molecules occurs within the exciton reservoir, with all emission occurring from the lower polariton branch. It will of course be interesting to explore the non-linear emission from such cavities to determine the extent to which hybridization can modify the process of polariton condensation.

Methods

Sample fabrication

BODIPY-Br and BODIPY-R were synthesized following procedures reported in the literature.^{25,26} The BODIPY-core materials Br and R were dispersed in a polystyrene (MW ~192.000) containing toluene solution at 35mg/ml, with the two BODIPY dyes (Br and R) having a relative mass fraction of 20% and 10% respectively. The PVA was dissolved in DI water at a concentration of 35mg/ml. The BODIPY-containing layers were spin-coated using 100 μ l of solution, with 150 μ l of solution used to deposit the PVA spacer layer. The thickness of each layer was controlled via spin-speed of the spin-coater. The thickness of each layer was measured on a Bruker DektakXT profilometer. The cavity silver mirrors were thermally evaporated using an Auto 306 Edwards thermal evaporator. Typical cavities had a Q-factor of 70.

Angular white-light reflectivity measurements

A Halogen-Deuterium white light source was used to illuminate the microcavities through the 35 nm semi-transparent silver mirror. The incident and reflected light was collimated and focused onto the sample and the detector respectively using lenses mounted on two moving arms. The two arms were connected to two concentric motorized wheels allowing us to change the angle of incidence between the white light source and the sample as well as the collection path. The reflected light was coupled into an optical fibre and imaged into an Andor Shamrock CCD spectrometer.

Angular PL and integrating sphere measurements

Angular dependent PL measurements were performed using the same collection path as described above. A fiber-coupled Fianium supercontinuum laser filtered at 500 nm by a SPEX 270M monochromator was used for non-resonant excitation of the microcavities through the semitransparent mirror. A laser beam was focused onto the samples with a slight downwards tilt to avoid direct reflection of the excitation beam into the CCD camera. Integrating sphere measurements were performed using a 405 nm CW laser diode to excite the microcavities. The cavity was placed inside the sphere, with a series of baffles placed inside the sphere to homogenise the optical field within the sphere. An optical fibre was used to collect the total PL from the integrating sphere exit port and

direct it to a CCD spectrometer. Black tape was placed around the edges of the cavity substrate to ensure that only light emitted from the front surface of the cavity was detected.

ASSOCIATED CONTENT

Supporting Information

The Supporting Information is available free of charge on the ACS Publications website at DOI:X.

Four level coupled oscillator model used and table of the values extracted from the model. Polariton PL conversion to polariton population density.

AUTHOR INFORMATION

Corresponding Author

*E-mail: d.g.lidzey@sheffield.ac.uk

ORCID

0000-0002-8558-1160

Funding

UK EPSRC via grant EP/M025330/1

Notes

The authors declare no competing financial interest.

ACKNOWLEDGMENTS

We thank the UK EPSRC for funding this research through the research grant EP/M025330/1 “Hybrid Polaritonics” and for funding a PhD scholarship for K.G.

REFERENCES

- (1) D. G. Lidzey; Bradley, D. D. C.; Skolnick, M. S.; Virgili, T.; Walker, S.; Whittaker, D. M. Strong Exciton-Photon Coupling in an Organic Semiconductor Microcavity. *Lett. to Nat.* **1998**, *395*, 53.
- (2) Lidzey, D. G.; Bradley, D. D. C.; Virgili, T.; Armitage, a.; Skolnick, M. S.; Walker, S. Room Temperature Polariton Emission from Strongly Coupled Organic Semiconductor Microcavities. *Phys. Rev. Lett.* **1999**, *82*, 3316.
- (3) Plumhof, J. D.; Stoeflerle, T.; Mai, L.; Scherf, U.; Mahrt, R. F. Room-Temperature Bose-Einstein Condensation of Cavity Exciton-Polariton in a Polymer. *Nat. Mater.* **2014**, *13*, 328.
- (4) Dietrich, C. P.; Steude, A.; Tropsch, L.; Schubert, M.; Kronenberg, N. M.; Ostermann, K.; Höfling, S.; Gather, M. C. An Exciton-Polariton Laser Based on Biologically Produced Fluorescent Protein. *Sci. Adv.* **2016**, *2*, e1600666.
- (5) Daskalakis, K. S.; Maier, S. a.; Murray, R.; Kéna-cohen, S. Nonlinear Interactions in an Organic Polariton Condensate. *Nat. Mater.* **2014**, *13*, 271.
- (6) Kéna-cohen, S.; Forrest, S. R. Room-Temperature Polariton Lasing in an Organic Single-Crystal Microcavity. *Nat. Photonics* **2010**, *4*, 371.
- (7) Daskalakis, K. S.; Maier, S. A.; Kéna-Cohen, S. Spatial Coherence and Stability in a Disordered Organic Polariton Condensate. *Phys. Rev. Lett.* **2015**, *115*, 35301.
- (8) Lerario, G.; Fieramosca, A.; Barachati, F.; Ballarini, D.; Daskalakis, K. S.; Dominici, L.; De Giorgi, M.; Maier, S. A.; Gigli, G.; Kéna-Cohen, S.; Sanvitto, D. Room-Temperature Superfluidity in a Polariton Condensate. *Nat. Phys.* **2017**, *13*, 837.
- (9) Cookson, T.; Georgiou, K.; Zasedatelev, A.; Grant, R. T.; Virgili, T.; Cavazzini, M.; Galeotti, F.; Clark, C.; Berloff, N. G.; Lidzey, D. G.; Lagoudakis, P. G. A Yellow Polariton Condensate in a Dye Filled Microcavity. *Adv. Opt. Mater.* **2017**, *5*, 1700203.
- (10) Imamoglu, A.; Ram, R.; Pau, S.; Yamamoto, Y. Nonequilibrium Condensates and Lasers without Inversion: Exciton-Polariton Lasers. *Phys. Rev. A* **1996**, *53*, 4250.
- (11) Lidzey, D. G.; Bradley, D. D. C.; Armitage, A.; Walker, S.; Skolnick, M. S. Photon-Mediated Hybridization of Frenkel Excitons in Organic Semiconductor Microcavities. *Science* **2000**, *288*, 1620.
- (12) Coles, D. M.; Somaschi, N.; Michetti, P.; Clark, C.; Lagoudakis, P. G.; Savvidis, P. G.; Lidzey, D. G. Polariton-Mediated Energy Transfer between Organic Dyes in a Strongly Coupled Optical Microcavity. *Nat. Mater.* **2014**, *13*, 712.
- (13) Zhong, X.; Chervy, T.; Wang, S.; George, J.; Thomas, A.; Hutchison, J. A.; Devaux, E.; Genet, C.; Ebbesen, T. W. Non-Radiative Energy Transfer Mediated by Hybrid Light-Matter States. *Angew. Chemie - Int. Ed.* **2016**, *55*, 6202.
- (14) Zhong, X.; Chervy, T.; Zhang, L.; Thomas, A.; George, J.; Genet, C.; Hutchison, J.; Ebbesen, T. W. Energy Transfer between Spatially Separated Entangled Molecules. *Angew. Chemie Int. Ed.* **2017**, *56*, 9034.
- (15) Jelley, E. E. Spectral Absorption and Fluorescence of Dyes in the Molecular State. *Nature* **1936**, *138*, 1009.
- (16) Scheibe, G. Der Chemie-Ingenieur. Ein Handbuch Der Physikalischen Arbeitsmethoden in Chemischen Und Verwandten Industrie- Betrieben. *Angew. Chem.* **1936**, *49*, 563.

- (17) Hobson, P. A.; Barnes, W. L.; Lidzey, D. G.; Gehring, G. A.; Whittaker, D. M.; Skolnick, M. S.; Walker, S. Strong Exciton-Photon Coupling in a Low-Q All-Metal Mirror Microcavity. *Appl. Phys. Lett.* **2002**, *81*, 3519.
- (18) Sundström, V.; Gillbro, T.; Gadonas, R. A.; Piskarskas, A. Annihilation of Singlet Excitons in J Aggregates of Pseudoisocyanine (PIC) Studied by Pico- and Subpicosecond Spectroscopy. *J. Chem. Phys.* **1988**, *89*, 2754.
- (19) Virgili, T.; Lidzey, D. G.; Bradley, D. D. C. Efficient Energy Transfer from Blue to Red in Tetraphenylporphyrin-Doped poly(9, 9-Dioctylfluorene) Light-Emitting Diodes. *Adv. Mater.* **2000**, *12*, 58.
- (20) Cerullo, G.; Stagira, S.; Zavelani-Rossi, M.; Silvestri, S. De; Virgili, T.; Lidzey, D. G.; Bradley, D. D. C. Ultrafast Förster Transfer Dynamics in Tetraphenylporphyrin Doped poly(9,9-Dioctylfluorene). *Chem. Phys. Lett.* **2001**, *335*, 27.
- (21) Scholes, G. D. Long-Range Resonance Energy Transfer in Molecular Systems. *Annu. Rev. Phys. Chem.* **2003**, *54*, 57.
- (22) Grant, R. T.; Michetti, P.; Musser, A. J.; Gregoire, P.; Virgili, T.; Vella, E.; Cavazzini, M.; Georgiou, K.; Galeotti, F.; Clark, C.; Clark, J.; Silva, C.; Lidzey, D. G. Efficient Radiative Pumping of Polaritons in a Strongly Coupled Microcavity by a Fluorescent Molecular Dye. *Adv. Opt. Mater.* **2016**, *4*, 1615.
- (23) Fontanesi, L.; Mazza, L.; La Rocca, G. C. Organic-Based Microcavities with Vibronic Progressions: Linear Spectroscopy. *Phys. Rev. B* **2009**, *80*, 235314.
- (24) Mazza, L.; Kéna-Cohen, S.; Michetti, P.; La Rocca, G. C. Microscopic Theory of Polariton Lasing via Vibronically Assisted Scattering. *Phys. Rev. B* **2013**, *88*, 75321.
- (25) Gupta, N.; Reja, S. I.; Bhalla, V.; Gupta, M.; Kaur, G.; Kumar, M. A Bodipy Based Dual Functional Probe for the Detection of Hydrogen Sulfide and H₂S Induced Apoptosis in Cellular Systems. *Chem. Commun.* **2015**, *51*, 10875.
- (26) Wang, Z.; Xie, Y.; Xu, K.; Zhao, J.; Glusac, K. D. Diiodobodipy-Styrylbodipy Dyads: Preparation and Study of the Intersystem Crossing and Fluorescence Resonance Energy Transfer. *J. Phys. Chem. A* **2015**, *119*, 6791.

Figures

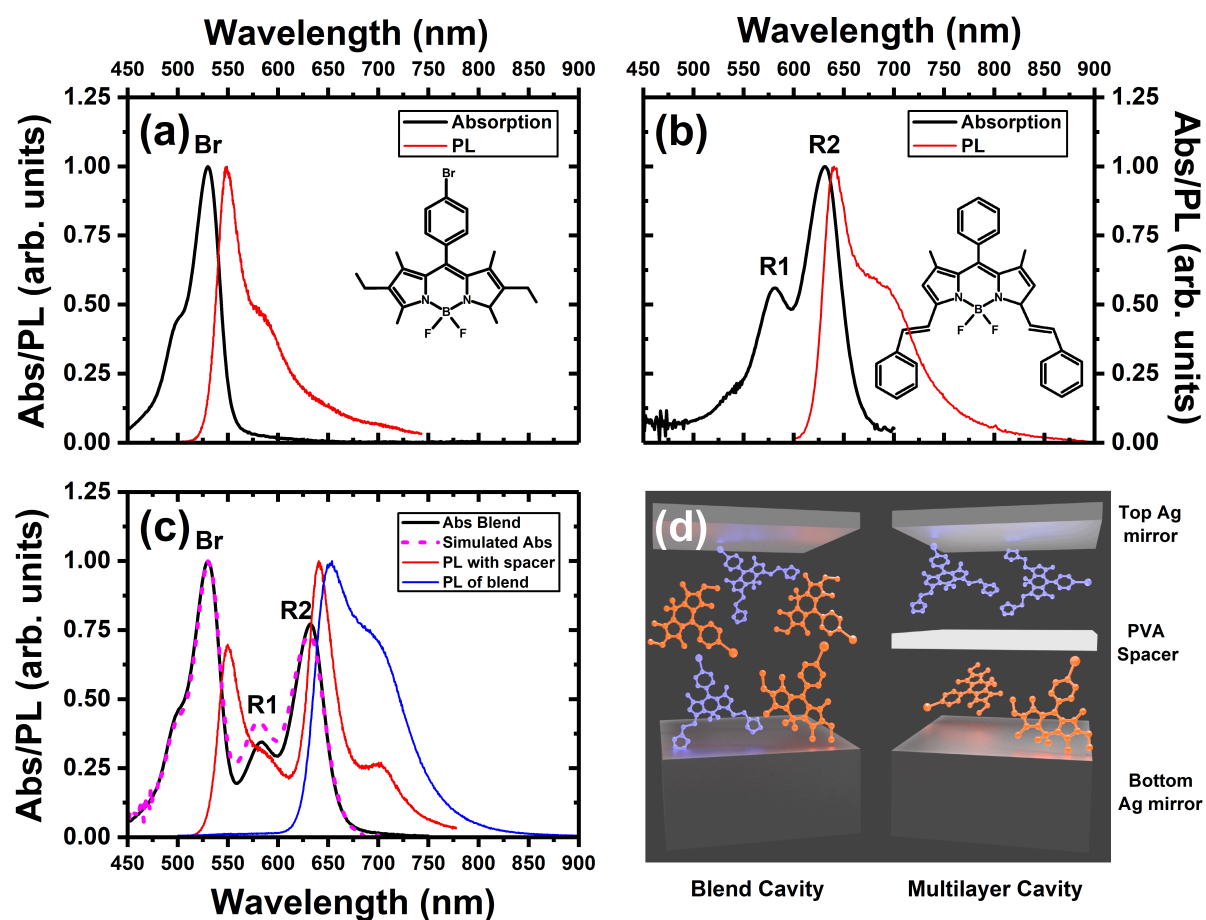


Figure 1. (a) Absorption and PL spectra of a BODIPY-Br control thin film along with its molecular structure. (b) Absorption and PL spectra of a BODIPY-R control thin film along with its molecular structure. (c) Absorption spectrum of the multilayer/blend film (black). PL emission from the multilayer (red) and blend (blue) thin film. Simulated absorption of the multilayer film (dotted) (d) Microcavity schematics for the two different configurations used (blend and multilayer).

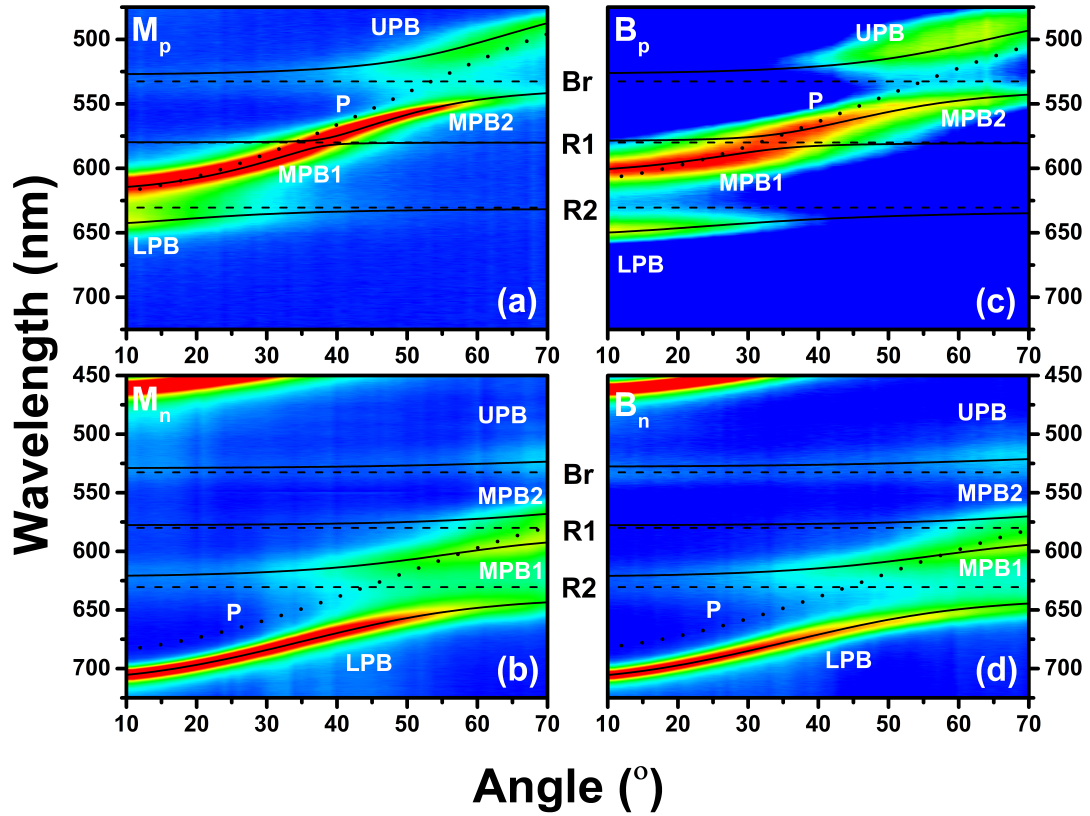


Figure 2. Angular white light reflectivity data from cavities (a) M_p , (b) B_p , (c) M_n and (d) B_n . The black solid lines represent the LPB, MPB1, MPB2 and UPB calculated using the four-level coupled oscillator model. The dashed and dotted lines show the energy of excitons Br, R1 and R2 and the cavity mode P of each cavity.

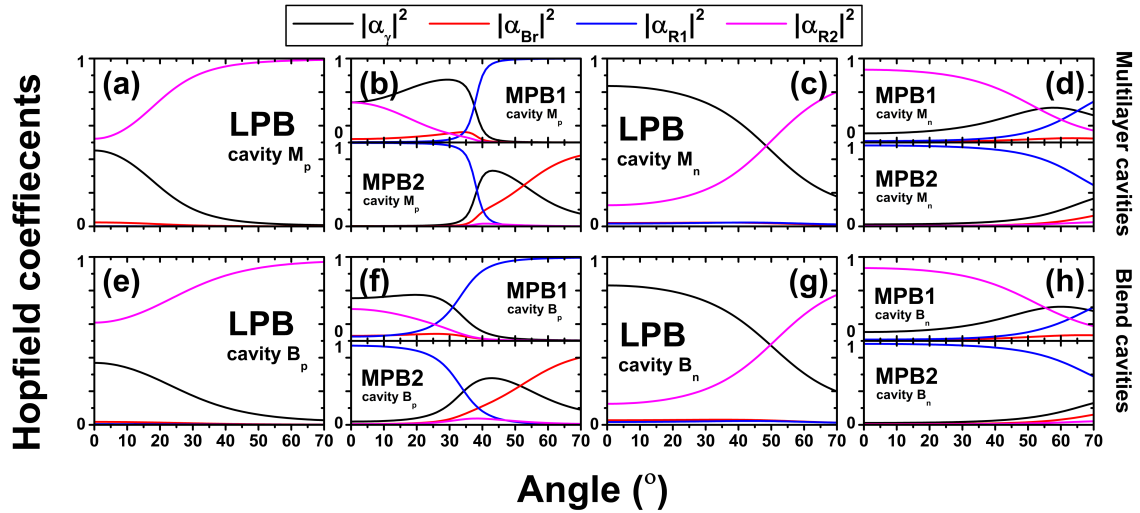


Figure 3. Hopfield coefficients of the LPB, MPB1 and MPB2 calculated using the four-level coupled oscillator model for multilayer cavities (a-b) M_p and (c-d) M_n and blend cavities (e-f) B_p and (g-h) B_n .

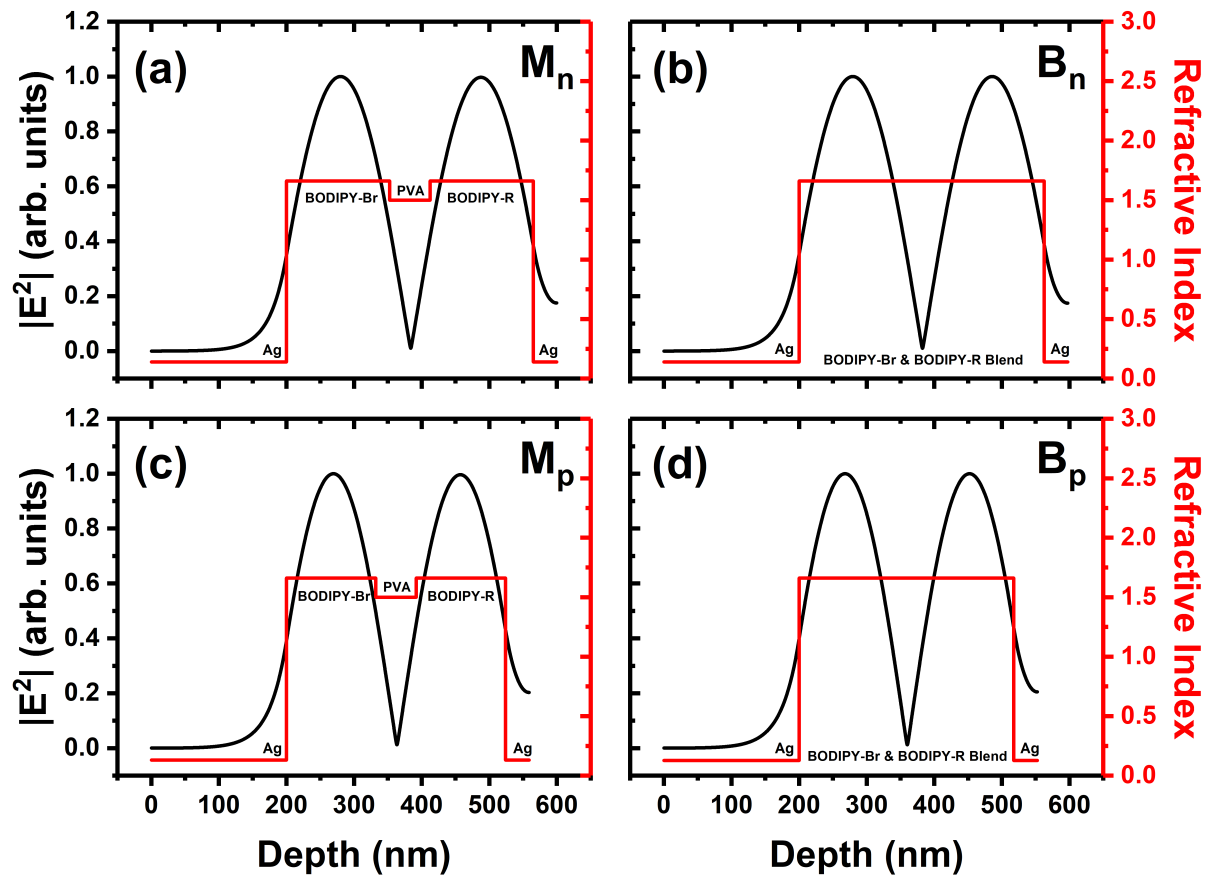


Figure 4. Electric field $|E^2|$ distribution and refractive index along the structure depth for the multilayer cavities (a) M_n and (c) M_p and the blend cavities (b) B_n and (d) B_p .

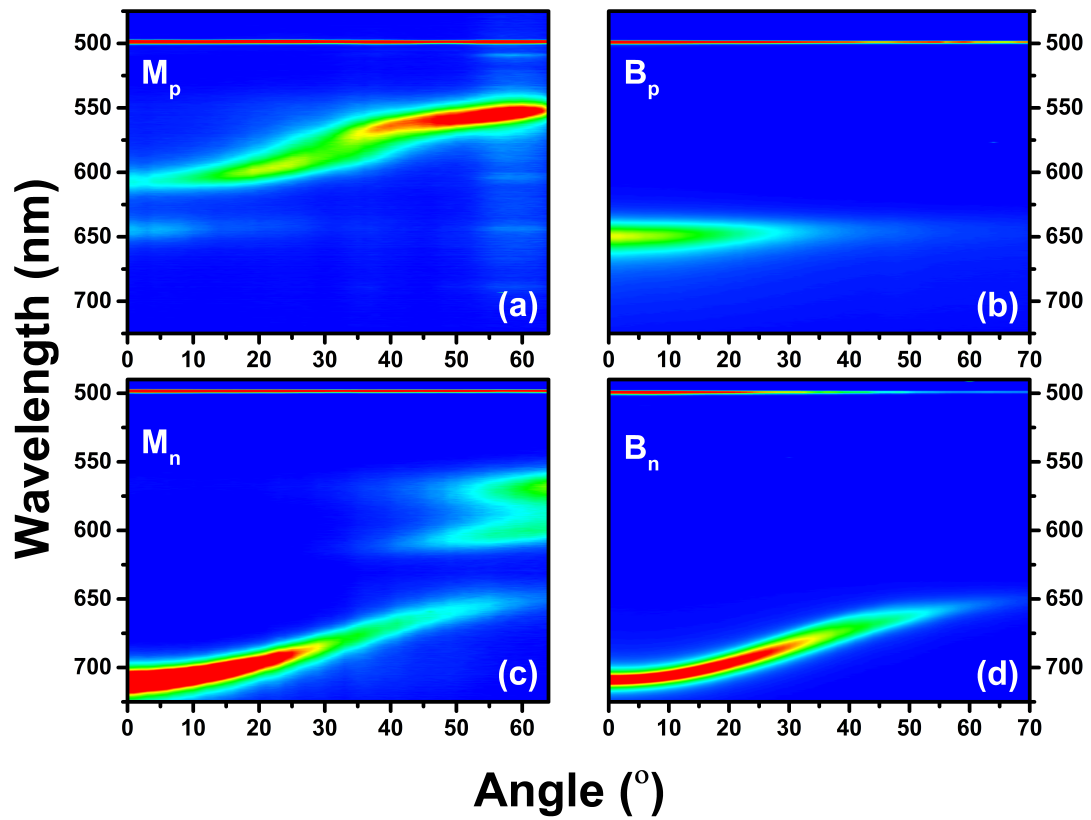


Figure 5. PL emission following non-resonant excitation at 500 nm. (a) Cavity M_p , (b) cavity B_p , (c) cavity M_n and (d) cavity B_n .

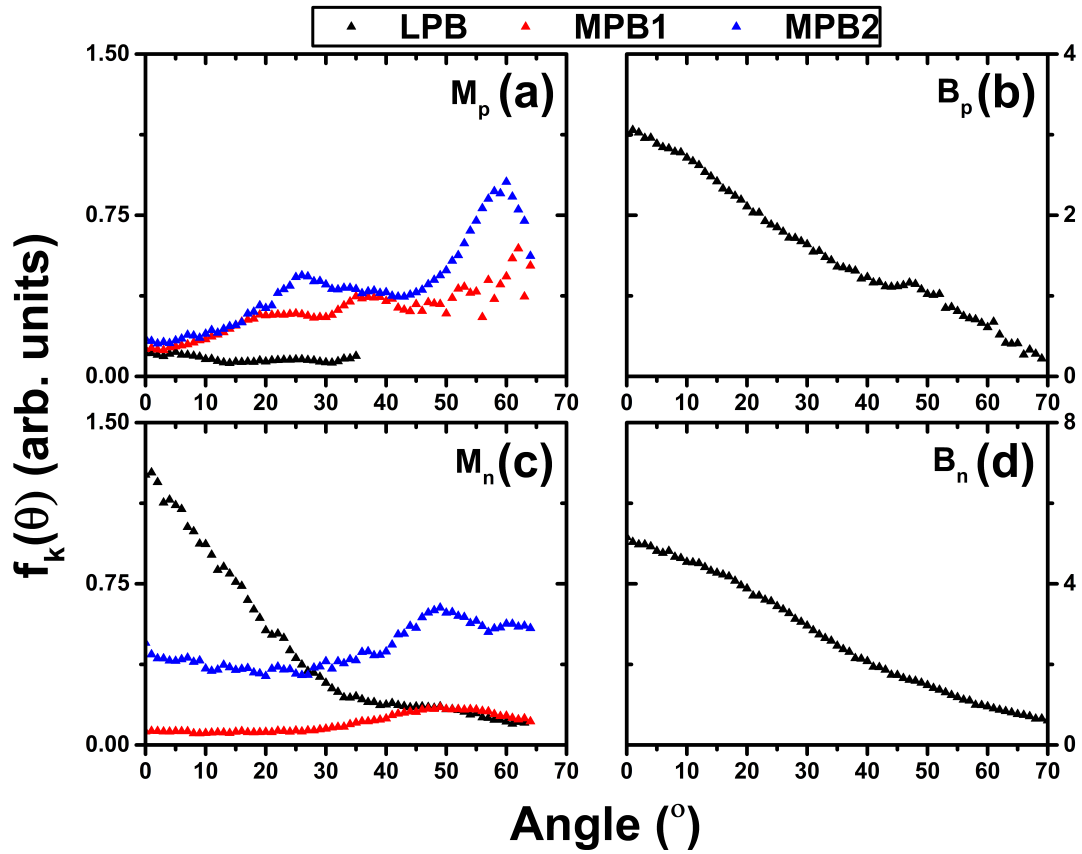


Figure 6. (a) Relative polariton population density $f_k(\theta)$ of LPB, MPB1 and MPB2 from cavity M_p (b) $f_k(\theta)$ of LPB from cavity B_p . (c) $f_k(\theta)$ of LPB, MPB1 and MPB2 from cavity M_n . (d) $f_k(\theta)$ of LPB from cavity B_n .

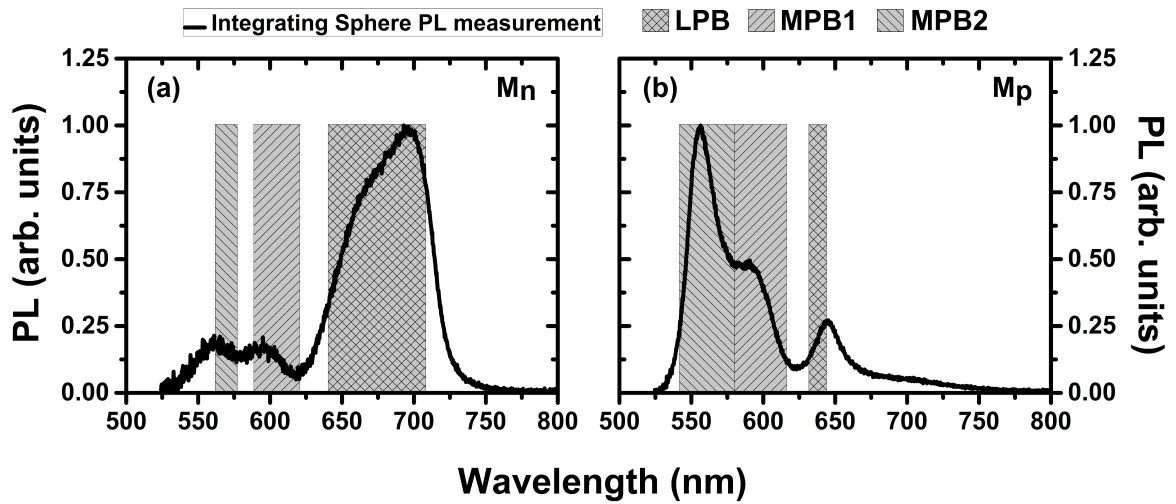
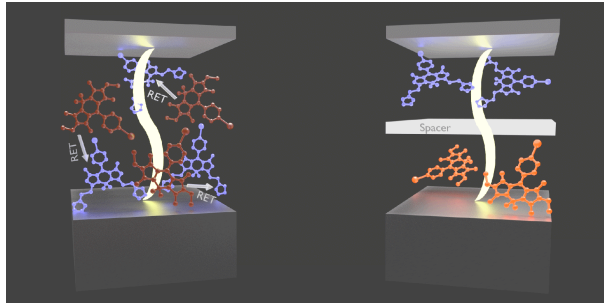


Figure 7. PL emission following non-resonant excitation at 405 nm using an integrating sphere. (a) Cavity M_n and (b) cavity M_p . The shaded area corresponds to the wavelength range of the LPB, MPB1 and MPB2.

For Table of Contents Use Only:

Control over energy transfer between fluorescent BODIPY dyes in a strongly-coupled microcavity.

Kyriacos Georgiou, Paolo Michetti, Lizhi Gai, Marco Cavazzini, Zhen Shen and David G. Lidzey



ToC: The two cavity configurations studied in this paper. One incorporating a film of the two fluorescent materials blended together and the other having the two materials separated by a PVA spacer. Here we schematically demonstrate that in the blended cavities the emission from the high-energy material is turned off due to Förster resonance energy transfer while in the multilayer cavity both molecules are bright.